



Insight into different adsorption behaviors of two fluoroquinolone antibiotics by sediment aggregation fractions

Bo Zhang¹ · Juan Chen¹ · Chao Wang¹ · Peifang Wang¹ · Ge Cui¹ · Jingjing Zhang¹ · Yu Hu¹ · Han Gao¹

Received: 15 July 2022 / Accepted: 28 October 2022 / Published online: 5 November 2022
© The Author(s), under exclusive licence to Springer-Verlag GmbH Germany, part of Springer Nature 2022

Abstract

Sediment, consisting of different aggregation fractions, is a hotspot site for transport and transformation of various pollutants including antibiotics. However, the fate of different antibiotics in aquatic sediments mediated by sediment aggregation fraction adsorption and the mechanism behinds are still unclear. In this study, we investigated the adsorption behavior of two fluoroquinolone antibiotics (ciprofloxacin and ofloxacin) on four aggregation fractions separated from the sediment of Taihu Lake, a typical lake contaminated by antibiotics in China. The results showed that the adsorption of ciprofloxacin and ofloxacin fitted the Freundlich model, irrespective of sediment aggregation size. The adsorption of ciprofloxacin and ofloxacin was depended on the size of sediment aggregation fractions, and the macroaggregation (> 200 μm) exhibited the strongest capacity, followed by large microaggregation (63–200 μm), medium microaggregation (20–63 μm), and small and primary microaggregation (< 20 μm). This fraction size-dependent effects of sediment aggregations on antibiotic adsorption might be closely related to the differences in their specific surface areas, organic matter contents, and surface functional groups. The adsorption of ciprofloxacin and ofloxacin by sediment aggregation fractions was characterized by a combination of chemical and physical adsorptions, with the former being the dominant process. Compared with ofloxacin, ciprofloxacin could be more rapidly and easily absorbed by four sediment aggregation fractions, and more readily complexed with carboxyl groups on macroaggregation surface. The adsorption of two antibiotics by extracellular polymeric substance showed that tryptophan and tyrosine protein-like, humic-like substance on the surface of sediment could bind to both antibiotics through a complexation reaction. The π - π electron donor–acceptor interaction and hydrogen bonds were responsible for the antibiotic adsorption by sediment aggregation.

Keywords Adsorption · Antibiotics · Extracellular polymeric substance · Sediment aggregation fraction

Highlights

- Antibiotics adsorption was depended on the size of sediment aggregation fractions.
- Sediment aggregation had a stronger affinity to ciprofloxacin than ofloxacin.
- Ciprofloxacin was complexed with carboxyl groups on macroaggregation surface.
- Antibiotics adsorption was by complexation, π - π electron interaction, and H bond.

Responsible Editor: Tito Roberto Cadaval Jr.

✉ Juan Chen
chenjuanmn@hhu.edu.cn

¹ Key Laboratory of Integrated Regulation and Resource Department On Shallow Lakes, Ministry of Education, College of Environment, Hohai University, 1 Xikang Road No.1 Jiangsu Province, Nanjing 210098, People's Republic of China

Introduction

Antibiotics have been substantially applied in human and veterinary medicine, agriculture, and aquaculture over a long term (Binh et al. 2018). The worldwide antibiotics consumption by humans witnessed an upsurge 2000 to 2015 from 21.1 to 34.8 billion doses per day, and the consumption is expected to rise to 40 billion doses per day by 2030 in the absence of policy intervention (Klein et al. 2018). Antibiotics can input the natural environments by wastewater discharges from hospitals, enterprise, agricultural, home, and livestock (Almeida et al. 2014; Parente et al. 2019). The adverse and chronic resistance of bacteria to antibiotics has ended up a potential risk to the fitness of human beings and animals (Kovalakova et al. 2020). Fluoroquinolones, a major class of antibiotics, has been widely used in human and veterinary medicine due to their wide activity spectrum against

bacteria and high efficiency in treating infectious diseases of urinary and respiratory systems (Dinh et al. 2017). Furthermore, fluoroquinolones are fluorinated compounds suggesting a higher potential for environmental persistence (Fadário et al. 2014). Ciprofloxacin (CPX) and ofloxacin (OFL) are two typical fluoroquinolones which have been increasingly detected in various aquatic ecosystems including lakes (Xu et al. 2014), river (Tang et al. 2019) and ocean (Li et al. 2018b). So far, the spatial distribution and potential health hazards of fluoroquinolones antibiotics in the environment have been extensively reported (Philip et al. 2018; Li et al. 2020), while the environmental behaviors and fates of antibiotics, especially their migration, transport and transformation, in aquatic ecosystems remain unclear.

Due to their large surface areas and high organic matter contents, sediment aggregation fractions have strong adsorption capacity to the antibiotics with high sediment–water partitioning coefficients (Tang et al. 2019). The antibiotics adsorbed on the sediment surface can migrate and transport in aquatic environment with the movement of sediment particles (e.g., entrainment, sedimentation, resuspension, etc.) (Hanamoto et al. 2018), which are directly related to their bioavailability and ecological risk (Aga et al. 2016). The size of sediment particle is a critical factor affecting the adsorption behaviors of organic pollutants (Luo et al. 2019). Generally, the small particles have a greater tendency to be suspended in water under wind wave disturbance (Sangster et al. 2015), resulting in greater exposure to antibiotics in water. In contrast, the larger particles more likely to settle and immobilize the adsorbed antibiotics (Fan et al. 2004). In addition to the weight differences, the structural and physicochemical characteristics of sediment, which are directly associated with adsorption capability (e.g., surface area, cation exchange capacity, organic matter content and surface functional group), also varied significantly among different aggregation fractions (Marttila and Kløve 2015). Studying the adsorption behavior and mechanism of antibiotics by different sediment aggregation fractions is essential to better understand their environmental fate in contaminated environments.

Beside sediment properties, physicochemical properties of antibiotics can impact the adsorption kinetic process (Siedlewicz et al. 2018). These two chemicals have different octanol–water partition coefficients ($\log K_{ow}$), molecular structure and acidity constants (pK_a) (Li et al. 2021a). The $\log K_{ow}$ of CPX (0.28) is known to be higher than that of OFL (-0.39) (Yang et al. 2020). These two antibiotics have similar chemical structure with one more -C-O- and two more -CH₃ on OFL, and one more -N(CH₂)₃ on CPX. The second acidity constants (pK_{a2}) for CPX and OFL are 8.7 and 8.3, respectively. Thus, it is reasonable to speculate that the adsorption process of

CPX and OFL by sediment aggregation fractions may be different, although they are in the same class of antibiotics. Given the fact that multiple pollutants coexist in a natural environment, the interactions of different antibiotics by competitive adsorptions on sediment aggregation fractions should be concerned. So far, most studies on sediment adsorption have focused on a single antibiotic (Maged et al. 2020; Shen et al. 2020), or investigated the interaction of antibiotic with metal cation in combined pollution systems (Zhao et al. 2013). Researches on the competitive adsorption of CPX and OFL on different sediment aggregation fractions are very limited and even less on the mechanisms behind.

In this study, we carried out three adsorption experiments, including adsorption kinetics, adsorption isotherm and competitive adsorption, to investigate the adsorption behaviors of CPX and OFL on four aggregation fractions separated from the sediment of Taihu Lake, one of the most antibiotic contaminated lakes in China. Fourier transform infrared (FTIR) spectroscopy and excitation-emission matrix combined with parallel factor (EEM-PARAFAC) analysis were used to further investigate the adsorption mechanism of antibiotics by non-fluorescent and fluorescent substances on different sediment aggregation fractions.

Materials and methods

Sediment aggregation preparation

Surface sediment (0–20 cm) sample was collected from the western area (31° 18' N, 119° 59' E) of Taihu Lake, China, with little human disturbance and antibiotic contamination (Li et al. 2021b). The fresh sediment was passed through an 8-mm sieve to remove any large plant debris and stones and was mixed thoroughly. The background concentrations of CPX and OFL in the sediment samples were below the detection limit. Prior to experiment, the sieved sediment was separated into four aggregation fractions with different sizes, that is, small and primary microaggregation (SPM, < 20 μm), medium microaggregation (MM, 20–63 μm), large microaggregation (LM, 63–200 μm), and macroaggregations (MAC, > 200 μm), using a sequence of sieves through wet-sieving (Six et al. 1998; Han et al. 2021). Initial chemical properties of four sediment aggregation fractions were determined, according to the methods described in Sect. 2.2, and the results are shown in Table S1. Each sediment aggregation fraction was freeze-dried and then was stored in a well-sealed polyethylene bottle before use (Siebers et al. 2018).

Freeze-dried sediments are used for antibiotic adsorption experiments, EPS extraction, and determination of physicochemical properties.

Sediment physicochemical properties analysis

Brunauer–Emmett–Teller surface area (BET) of sediment aggregation fractions was measured using a BET-N₂ surface area analyzer (V-Sorb 2800TP, Gold APP, China). Total organic carbon (TOC) content of the sediment aggregation fractions was measured using the K₂CrO₇-H₂SO₄ oxidation method. Total nitrogen (TN) content was determined after acid digestion according to the Kjeldahl digestion method (Zheng et al. 2018). Total phosphorus (TP) content was measured following the methods of Chen et al. (2020). Cation-exchange capacity (CEC) was determined using an ammonium acetate solution at pH 7.0. An X-ray diffraction (XRD) (Ultima IV, Rigaku, Smart Lab) was used to determine the chemical compositions of sediment aggregation fractions before adsorption experiments. A Cu K α radiation was adopted in a range of 10° to 80° under the operating condition of 40 kV and 100 mA. Scanning electron microscopy (SEM) (S-4800, Hitachi, Japan) images of four sediment aggregation fractions had been taken under a microscope at 3.0 kV.

Antibiotic adsorption experiments of four sediment aggregation fractions

Four antibiotic adsorption experiments of four sediment aggregation fractions, including adsorption kinetics, adsorption isotherm, competitive adsorption, and temperature effect experiment, were conducted using glass centrifuge tubes with a total volume of 50 mL. The CPX or OFL (purchased from Sigma Chemicals, purity > 99%) was dissolved in 0.01 M CaCl₂. Then, 40 mL of antibiotic solution with the concentration described below and 0.1 g of each sediment aggregation fraction was added into the tube, and placed in a shaker (MQS-30, MinQuan Instrument, China) in dark with a speed of 120 rpm at 25 °C. For the adsorption kinetics experiment, the tubes containing antibiotic solution (with the CPX or OFL concentration of 40 mg·L⁻¹) and sediment aggregation fraction were shaken for 0, 0.5, 1, 2, 4, 8, 12, and 24 h. For the adsorption isotherm experiment, the CPX or OFL solution with eight concentrations (0, 1, 2, 4, 8, 10, 20, 30, and 40 mg·L⁻¹) and sediment aggregation fraction were added into the tubes, and then were shaken for 24 h. For the competitive adsorption experiment, a mixture of CPX and OFL at a ratio of 1:1 (with respective concentration of 1, 2, 5, 15, and 25 mg·L⁻¹) and sediment aggregation fraction were added into the tubes, and then were shaken for 24 h. For the effect of temperature experiment,

40 mL of solution with different concentrations of CPX and OFL under different temperature (288.15, 298.15 and 308.15 K) controlled shaker at 120 rpm for 24 h. All experiments were conducted in triplicate. At each sampling time, the supernatant in each tube was collected after centrifugation at 4000 rpm for 10 min, and then was stored in a brown glass bottle with a cap for the subsequent determination of CPX and OFL concentrations. At the end of the adsorption kinetics experiments, the sediment aggregation fraction settling at the bottom of the tube was collected, freeze-dried, and stored in a polyethylene centrifuge tube for the subsequent FTIR analysis. An FTIR spectroscopy (Nicolet iS50, Thermo Scientific, USA) was used to identify the surface functional groups of four sediment aggregation fractions. The FTIR spectra were obtained in transmission mode in the wavelength range of 1000–4000 cm⁻¹ with a resolution of 4 cm⁻¹ and 32 repetitive scans.

Antibiotic concentration analysis

The supernatant samples obtained from sediment aggregation fraction adsorption experiments were passed through 0.22- μ m polytetrafluoroethylene membranes, and then the CPX and OFL concentrations in the filtered water sample were determined using an ultra-performance liquid chromatography-tandem mass spectrometer (UPLC-MS) (ACQUITY UPLC Xevo TQ, Waters, USA) equipped with an ACQUITY BEH C18 column (100 mm \times 2.1 mm, i.d. 1.7 μ m). The mobile phases were according to the method of Yu et al. (2019) with slight modification, that is, phase A: water (0.05% formic acid), phase B: acetonitrile, with the flow rate of 0.4 mL·min⁻¹. The gradient program was as follows: (i) the fluent was injected into a flow of 90%: 10% (A: B) and maintained for 2 min; (ii) increased to 95% (B) by 2 min; maintained 95% (B) until 3 min; (iii) reduced to 10% (B) by 3 min and maintained at 90%: 10% (A: B) until 4 min. Detailed information for the MS analysis of CPX and OFL (e.g., ion mode, precursor ion, production ion, cone voltage and collision energy) are shown in Table S2. The standard calibration curves were calculated using a series of individual antibiotic samples with concentrations of 1, 5, 10, 50, 100, and 200 μ g·L⁻¹ ($R^2 > 0.999$). Details about the quality control of the method are shown in Supplementary Information.

Antibiotic adsorption experiments of extracellular polymeric substance

The extracellular polymeric substance (EPS) of four sediment aggregation fractions (0.1 g) were extracted according to the methods of Yang et al. (2018). The adsorption

experiments of CPX and OFL to EPS were conducted under the same conditions as adsorption isotherm experiment described in Sect. 2.3. Afterwards, the solution which was collected after centrifugation at 4000 rpm for 10 min storing at 4 °C for the subsequent excitation-emission matrix (EEM) fluorescence analysis.

EEM fluorescence was measured using three-dimensional spectrofluorometer (F-7000, Hitachi, Japan). The emission and excitation wave-lengths both scan from 250 to 550 nm at 5 nm increments. All EEM fluorescence results were corrected with a water blank and converted to Raman units (R.U.) by normalizing the area under the Milli-Q Raman scatter peak the Raman peak (Ex = 350 nm, Em = 381–426 nm). Prior to analysis, the Raman and Rayleigh scatters were removed according to Stedmon and Bro (2008).

A parallel factor (PARAFAC) analysis was used to remove the overlapping fluorescence peaks and decompose the EEM into individual components through drEEM toolbox in MATLAB software (MATLAB®R2014a, Natick, USA). The PARAFAC was computed using two to five component models with non-negativity constraints, and then residual analysis, split-half analysis, and visual inspection were applied to determine the number of fluorescence components (Huang et al. 2018). It is assumed that the maximal fluorescence intensity (F_{\max}) of individual fluorescent components is proportional to the real concentrations of the corresponding fluorescent components (Gu et al. 2017).

Data analysis

The adsorption content of four sediment aggregation fraction on antibiotics was obtained by the residual concentration of antibiotics (Eq. (1)).

$$Q = \frac{(C_0 - C_e) * V}{m} \quad (1)$$

where C_0 and C_e ($\text{mg}\cdot\text{L}^{-1}$) are the initial and equilibrium aqueous phase CPX and OFL concentrations for two antibiotics (CPX and OFL), respectively; V (L) is the volume of aqueous added; m (g) is the weight of four sediment aggregation fractions; Q ($\text{mg}\cdot\text{g}^{-1}$) is the adsorption content of four sediment aggregation fractions on antibiotics.

Pseudo-first-order model (Eq. (2)), pseudo-second-order model (Eq. (3)), intraparticle diffusion model (Eq. (4)) were used to clarify the adsorption kinetics of CPX and OFL on the sediment aggregation fractions.

$$\ln(q_e - q_t) = \ln q_e - k_1 t \quad (2)$$

$$\frac{1}{q_t} = \frac{1}{k_2 q_e^2} + \frac{1}{q_e} t \quad (3)$$

$$q_t = k_{diff} t^{0.5} + C \quad (4)$$

where q_e ($\text{mg}\cdot\text{g}^{-1}$) and q_t ($\text{mg}\cdot\text{g}^{-1}$) are the equilibrium sorption capacity and at the time (t); k_1 (h^{-1}) and k_2 ($(\text{g}\cdot\text{mg}^{-1})\cdot\text{h}^{-1}$) are the rate constants for pseudo-first-order and pseudo-second-order model kinetic models, respectively; k_{diff} ($(\text{mg}\cdot\text{g}^{-1})\cdot\text{h}^{0.5}$) is the intraparticle diffusion rate constant and C is a constant related to the boundary layer thickness.

The Langmuir (Eq. (5)) and Freundlich (Eq. (6)) isotherm models were used to clarify the adsorption characteristics of CPX and OFL on sediment aggregation fractions.

$$Q_e = Q_m \frac{K_L C_e}{1 + K_L C_e} \quad (5)$$

$$Q_e = K_F C_e^{\frac{1}{n}} \quad (6)$$

where Q_e ($\text{mg}\cdot\text{g}^{-1}$) is the equilibrium sorption capacity; C_e ($\text{mg}\cdot\text{L}^{-1}$) is the equilibrium aqueous phase CPX and OFL concentrations; Q_m ($\text{mg}\cdot\text{g}^{-1}$) is the maximum adsorption capacity under monolayer adsorption; K_L is the affinity coefficient of Langmuir model; K_F is Freundlich's affinity coefficient and n is the empirical constant of Freundlich model.

Thermodynamic parameters (ΔG) ($\text{kJ}\cdot\text{mol}^{-1}$) were calculated from following equations (Tan et al. 2013):

$$\Delta G = -RT \ln K \quad (7)$$

The enthalpy change (ΔH) ($\text{kJ}\cdot\text{mol}^{-1}$) and entropy changes (ΔS) ($\text{kJ}\cdot(\text{K}\cdot\text{mol})^{-1}$) for adsorption process were calculated using the following equations:

$$\ln K = \frac{\Delta S}{R} - \frac{\Delta H}{RT} \quad (8)$$

where R , T , and K are the universal gas constant ($8.314 \text{ J}\cdot(\text{K}\cdot\text{mol})^{-1}$), the absolute temperature (K) and the equilibrium constant, respectively. ΔH and ΔS could be calculated from the slope and intercept of the linear plot of $\ln K$ versus $1/T$.

Model fitting of the kinetic and isothermal adsorption data was carried out and the corresponding adsorption parameters were obtained using Origin 8.0 software (OriginLab Corporation, Northampton, USA). The data were tested for the normality and variance assumptions of the parametric ANOVA. The differences in physico-chemical properties of sediment aggregation fractions (BET, CET, TN, TP, and TOC) were determined by a one-way analysis of variance (ANOVA). For the competitive

adsorption experiment, significant differences between antibiotic concentrations were detected with the one-way ANOVA followed by a Tukey's test and Student's *t*-test was used to determine the differences between antibiotic types. All *p* values below 0.05 were considered statistically significant. A Spearman's correlation analysis was used to determine the correlations between the obtained adsorption parameters (K_L and K_F) and physicochemical properties of four sediment aggregation fractions (TOC, CEC, BET, TN, TP). The above analyses were performed using the SPSS 25.0 software package (SPSS Inc., Chicago, IL., USA).

Results and discussion

Physicochemical properties of sediment aggregation fractions

As shown in Table S1, the sediment properties including TN, TP, and TOC differed significantly among four sediment aggregation fractions, and their concentrations decreased in the following order: MAC > LM > MM > SPM. The CEC of LM and MAC was approximately threefold higher than that of SPM and MM. The BET values of four sediment aggregation fractions ranged from 19.83 m²·g⁻¹ (MAC) to 8.45 m²·g⁻¹ (SPM). The MAC showed the highest BET, probably due to that it had highest TOC content than other fractions (Table S1) and porous surface (Fig. 1). Zhao et al. (2018)

reported the TOC content showed a positive correlation with BET surface area. The XRD patterns of four sediment aggregation fractions are shown in Fig. 2. The peaks that appeared in the XRD patterns of SPM and MM correspond to two crystalline structures, matching with quartz-SiO₂ (PDF#85–0796) and berlinite-AlPO₄ (PDF#76–0228). Only quartz-SiO₂ (PDF#85–0796) was identified in the XRD pattern of LM, and no crystalline phase was observed in MAC. This indicated that the chemical compositions were distinct significantly among four sediment aggregation fractions.

Adsorption kinetics of CPX and OFL on different sediment aggregation fractions

The pseudo-second-order and pseudo-first-order model fitting results of the adsorption kinetics for CPX and OFL onto different sediment aggregation fractions are shown in Fig. 3. The adsorption process of four sediment aggregation fractions to CPX and OFL included two stages, that is, rapid adsorption and adsorption equilibrium. The rapid adsorption phase occurred before the beginning of 1 h. The adsorption reached equilibrium approximately at 8 h for all sediment aggregation fractions. A reason for this phenomenon was that a great number of adsorption sites on sediment surfaces increase the frequency of contact between antibiotics and sediment particles at the beginning of the adsorption process (Huang et al. 2020), resulting in the rapid adsorption of the antibiotic. Subsequently, the adsorption sites on sediment

Fig. 1 Images of scanning electron microscopy for small and primary microaggregation (A), medium microaggregation (B), large microaggregation (C) and microaggregation (D)

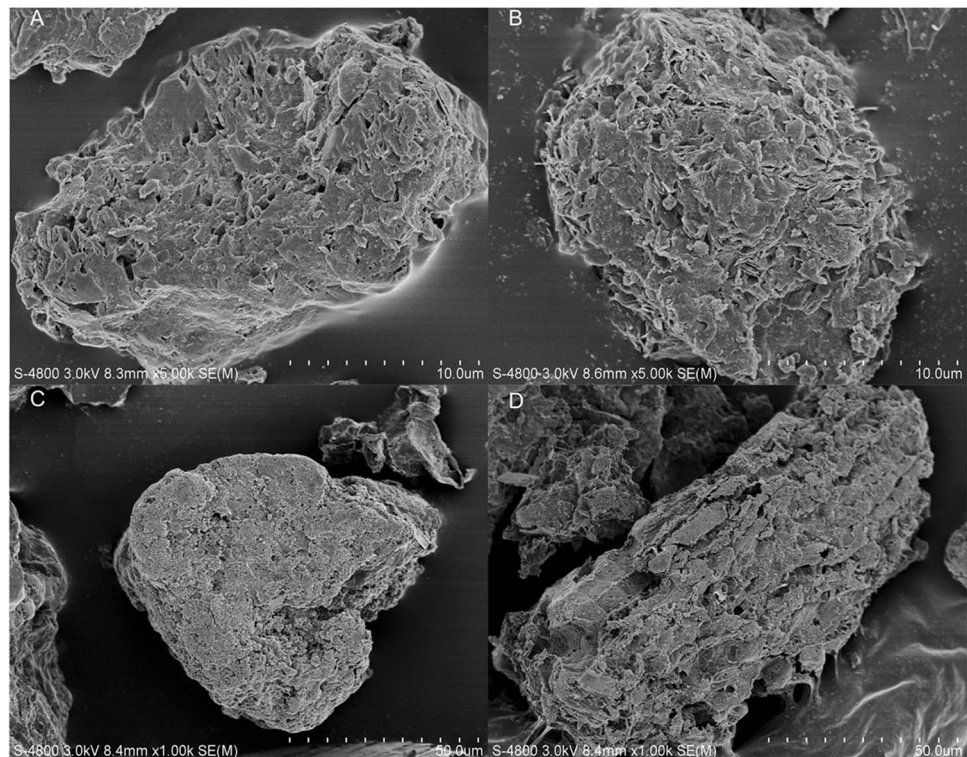


Fig. 2 X-ray diffraction patterns of four sediment aggregation fractions separated from the Taihu Lake (SPM: small and primary microaggregation, MM: medium microaggregation, LM: large microaggregation, MAC: microaggregation)

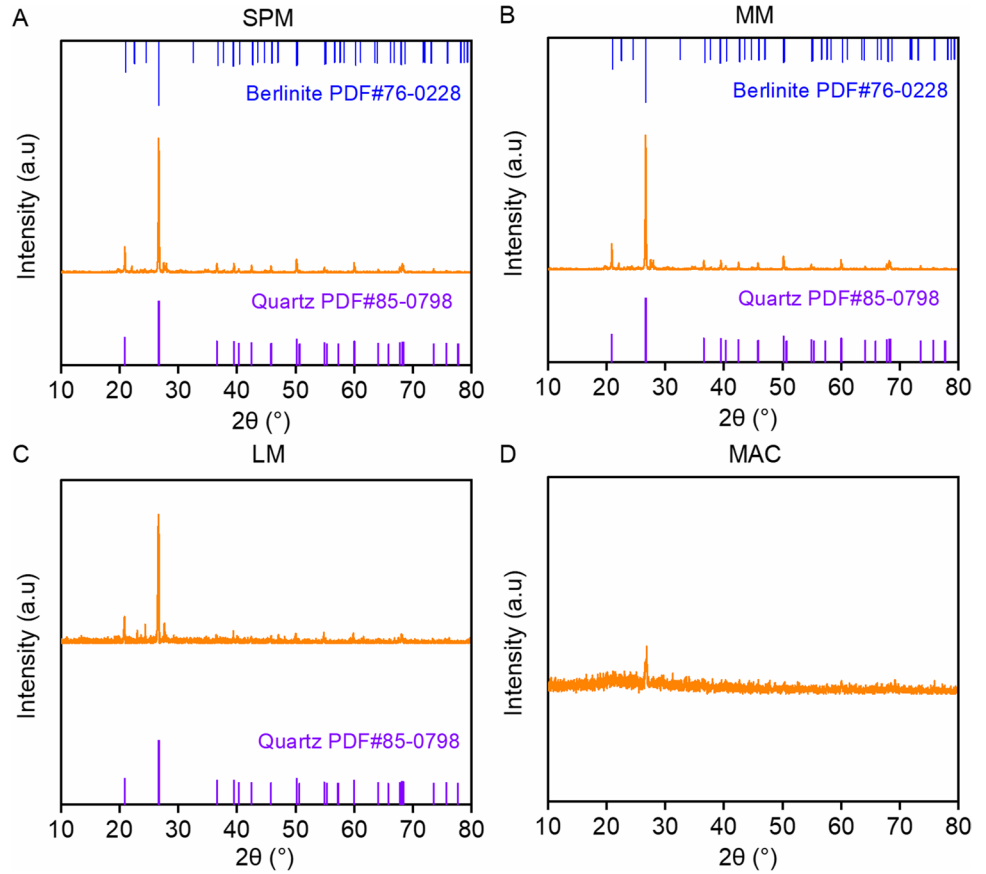
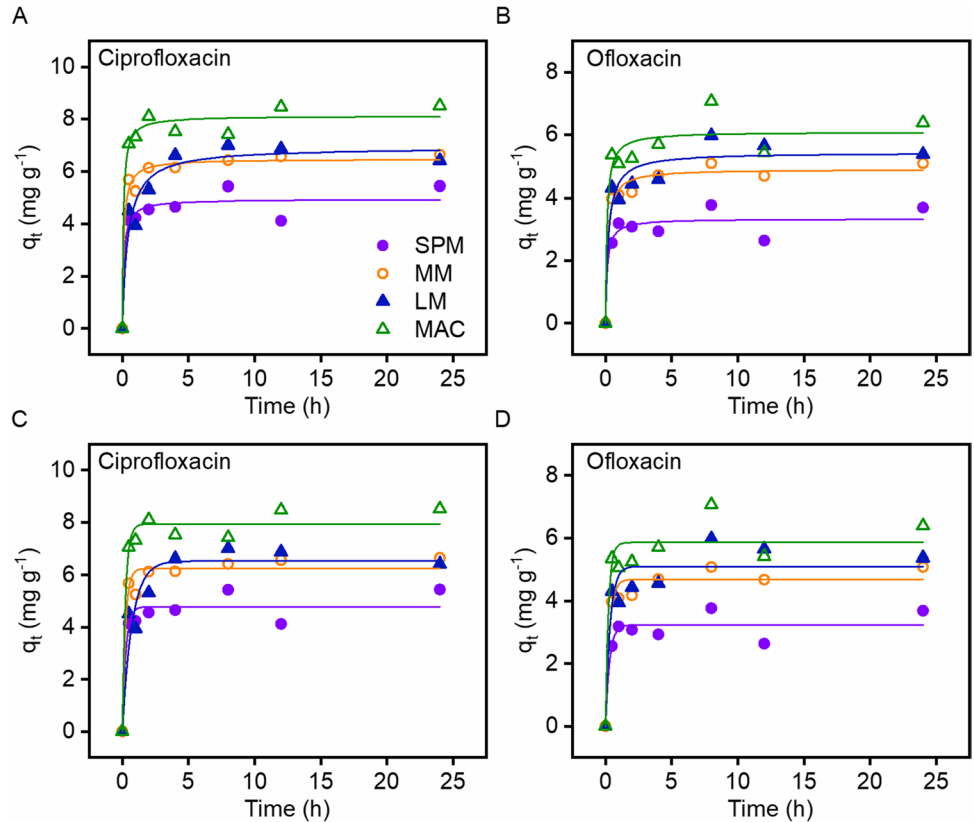


Fig. 3 Pseudo-second-order kinetic model (A, B) and pseudo-first-order kinetic model (C, D) fitting the kinetic adsorption of ciprofloxacin and ofloxacin on four sediment aggregation fractions (SPM: small and primary microaggregation, MM: medium microaggregation, LM: large microaggregation, MAC: microaggregation)



surfaces might be gradually saturated as the adsorption time increased, and the driving force in the solution transferred antibiotic molecules to the sediment surface. Then the antibiotic molecules slowly reached internal active sites under the mass transfer force, and gradually occupied the sites, reaching adsorption equilibrium (Cao et al. 2017; Hu et al. 2020; Li et al. 2022).

The adsorption kinetics model fitting results and kinetic parameters of each kinetic model are listed in Table 1. The adsorptions of two antibiotics onto sediments, irrespective of fraction size, were well-fitted to the pseudo-second-order kinetic model, with the regression coefficients (R^2) ranging from 0.903 to 0.984. In contrast, the pseudo-first-order and intraparticle diffusion models showed poor fits for the CPX and OFL adsorptions on sediments. The pollutant adsorptions matching pseudo-second-order kinetic model have been considered to be mainly controlled by chemical interactions (Arshadi et al. 2018; Soltani et al. 2018). Based on the fitting result of the pseudo-second-order model, the adsorption capacity could be affected by both the antibiotic type and the sediment aggregation size (Table 1). Compared with OFL (q_e , 3.335–6.091 mg·g⁻¹), CPX (q_e , 4.951–8.118 mg·g⁻¹) was more easily adsorbed onto four sediment aggregation fractions. This might be due to that the CPX (log K_{ow} 0.28) has stronger lipophilicity than OFL (log K_{ow} -0.39) (Yang et al. 2020). Among four sediment aggregation fractions, the MAC exhibited the highest adsorption capacity (q_e) for both CPX and OFL, and followed by LM, MM and SPM, which was in line with the results of sediment BET, CEC, and TOC contents (Table S1). As shown in Table S3, sediment CEC, BET, and TOC contents were significantly positively correlated with q_e of CPX and OFL adsorptions. Sediment aggregation fractions with higher BET and CEC indicate that they have more adsorption sites on the surfaces (Wu and Zhou 2019), probably positively contributing to the antibiotic adsorption.

Adsorption isotherms of CPX and OFL on different sediment aggregation fractions

Isothermal adsorption curves, characterizing the relationships between adsorption amount and adsorption concentration at a constant temperature, have been widely used to clarify the interaction relationships between active sites and adsorbate (Zhu et al. 2017; Xiong et al. 2021). As shown in Fig. 2, the saturated adsorption capacities (Q_e), irrespective of sediment aggregation fraction size, were gradually increased with the increasing equilibrium concentrations (C_e) of CPX or OFL. Different sediment aggregation fractions could remove around 90% when CPX and OFL concentration was 1.0 mg·L⁻¹ (Fig. S3). The removal efficiency decreased gradually with the increase of concentration. MAC had the highest removal efficiency at all concentrations.

The fitting results of Langmuir and Freundlich isothermal adsorption models are shown in Table 2. According to the fitting coefficient (R^2) of Freundlich model for each sediment aggregation fraction was slightly higher than that of Langmuir model, for both CPX and OFL. In the Freundlich model, the parameter n indicates the reactivity and heterogeneity of active sites of the adsorbent (Aljeboree et al. 2017). When $n = 1$ the adsorption is linear; when $n > 1$ the adsorption is considered to be higher energy adsorption dominated by chemical processes; and when $n < 1$ there are heterogeneous sites of high adsorption energy dominated by physical processes (Pezoti et al. 2014). The n values were larger than 1 in the Freundlich model of CPX and OFL adsorption on four sediment aggregation fractions, indicating that high energy active sites on sediments may have strong bonding capability to CPX and OFL via a chemical process. The K_F parameter of Freundlich model for CPX and OFL adsorption showed in Table 2, which is related to the adsorption capacity in multilayer (Conde-Cid et al. 2019).

Table 1 Kinetic parameters for the adsorption of ciprofloxacin and ofloxacin onto four sediment aggregate fractions separated from the Taihu Lake

Antibiotic	Sediment fraction	$q_{e,exp}$ (mg·g ⁻¹)	First-order kinetic			Second-order kinetic			Intraparticle diffusion		
			q_e (mg·g ⁻¹)	k_1 (h ⁻¹)	R^2	q_e (mg·g ⁻¹)	k_2 (g·(mg·h) ⁻¹)	R^2	k_{diff} (mg·(g·h ^{0.5}) ⁻¹)	C	R^2
Ciprofloxacin (CPX)	SPM (<20 μm)	4.653	4.784	3.630	0.926	4.951	1.675	0.939	0.243	4.089	0.410
	MM (20–63 μm)	6.419	6.242	4.121	0.966	6.468	1.421	0.984	0.286	5.450	0.729
	LM (63–200 μm)	6.856	6.541	1.338	0.910	6.914	0.339	0.946	0.601	4.404	0.545
	MAC (>200 μm)	8.464	7.928	4.123	0.975	8.118	1.462	0.981	0.304	7.058	0.600
Ofloxacin (OFL)	SPM (<20 μm)	3.192	3.236	3.221	0.903	3.335	2.322	0.903	0.160	2.751	0.261
	MM (20–63 μm)	5.083	4.695	3.320	0.960	4.898	1.353	0.981	0.267	3.920	0.753
	LM (63–200 μm)	5.371	5.111	2.799	0.887	5.431	0.823	0.932	0.397	3.970	0.604
	MAC (>200 μm)	5.696	5.850	4.341	0.911	6.091	1.437	0.930	0.293	5.060	0.371

Table 2 Fitting results of Freundlich and Langmuir isotherm models of ciprofloxacin and ofloxacin adsorption onto four sediment aggregate fractions separated from the Taihu Lake (K_F : Freundlich coefficient, n : Freundlich empirical, K_L : Langmuir coefficient)

Antibiotic	Sediment fraction	T (K)	Freundlich			Langmuir		
			K_F	n	R^2	Q_m	K_L	R^2
Ciprofloxacin (CPX)	SPM (< 20 μm)	288.15	1.204	4.632	0.929	2.271	1.472	0.775
	MM (20–63 μm)		1.451	3.184	0.882	4.685	0.212	0.745
	LM (63–200 μm)		2.099	4.122	0.865	4.331	1.541	0.983
	MAC (> 200 μm)		2.249	3.563	0.948	5.218	0.897	0.938
	SPM (< 20 μm)	298.15	1.534	3.404	0.956	3.906	0.588	0.921
	MM (20–63 μm)		1.604	2.409	0.980	5.901	0.326	0.963
	LM (63–200 μm)		1.891	2.081	0.918	8.203	0.271	0.913
	MAC (> 200 μm)		2.834	2.667	0.956	7.498	0.792	0.914
	SPM (< 20 μm)	308.15	3.708	2.892	0.953	9.785	0.575	0.857
	MM (20–63 μm)		2.700	1.899	0.884	20.769	0.081	0.848
	LM (63–200 μm)		2.877	1.797	0.988	15.263	0.198	0.958
	MAC (> 200 μm)		3.132	2.032	0.829	12.819	0.275	0.780
Ofloxacin (OFL)	SPM (< 20 μm)	288.15	1.346	4.749	0.922	2.705	0.769	0.873
	MM (20–63 μm)		1.017	3.118	0.925	3.028	0.408	0.956
	LM (63–200 μm)		1.092	3.357	0.918	3.048	0.394	0.901
	MAC (> 200 μm)		1.805	4.545	0.904	3.343	2.276	0.867
	SPM (< 20 μm)	298.15	1.149	2.938	0.963	3.359	0.427	0.960
	MM (20–63 μm)		1.249	2.193	0.974	5.344	0.253	0.986
	LM (63–200 μm)		1.239	2.125	0.992	5.688	0.217	0.975
	MAC (> 200 μm)		2.299	2.969	0.851	5.909	0.717	0.915
	SPM (< 20 μm)	308.15	2.846	2.987	0.973	7.530	0.729	0.964
	MM (20–63 μm)		2.057	1.788	0.941	12.298	0.182	0.957
	LM (63–200 μm)		2.289	2.069	0.973	10.708	0.218	0.936
	MAC (> 200 μm)		2.543	1.865	0.938	14.684	0.152	0.894

To reveal the possible effects of sediment aggregation fraction properties on antibiotic adsorption, we analyzed the correlations between sediment aggregation fraction physicochemical properties (BET, CEC, TN, TP, and TOC) and adsorption capacity parameters (K_F for CPX and OFL). As shown in Table S3, sediment CEC, BET, and TOC contents were significantly positively correlated with adsorption capacity parameters of CPX and OFL adsorptions ($p < 0.01$). The positive effects of TOC and CEC on adsorption capacity may due to the specific sites containing a large number of adsorbed antibiotics in organic matter (Scherr et al. 2009), cation exchange and ionic bridging abilities (Rath et al. 2019), respectively. Qi et al. (2014) reported that the adsorption capacity of agricultural soils to estrogen was limited by the number of adsorption sites distributed on soil organic matter.

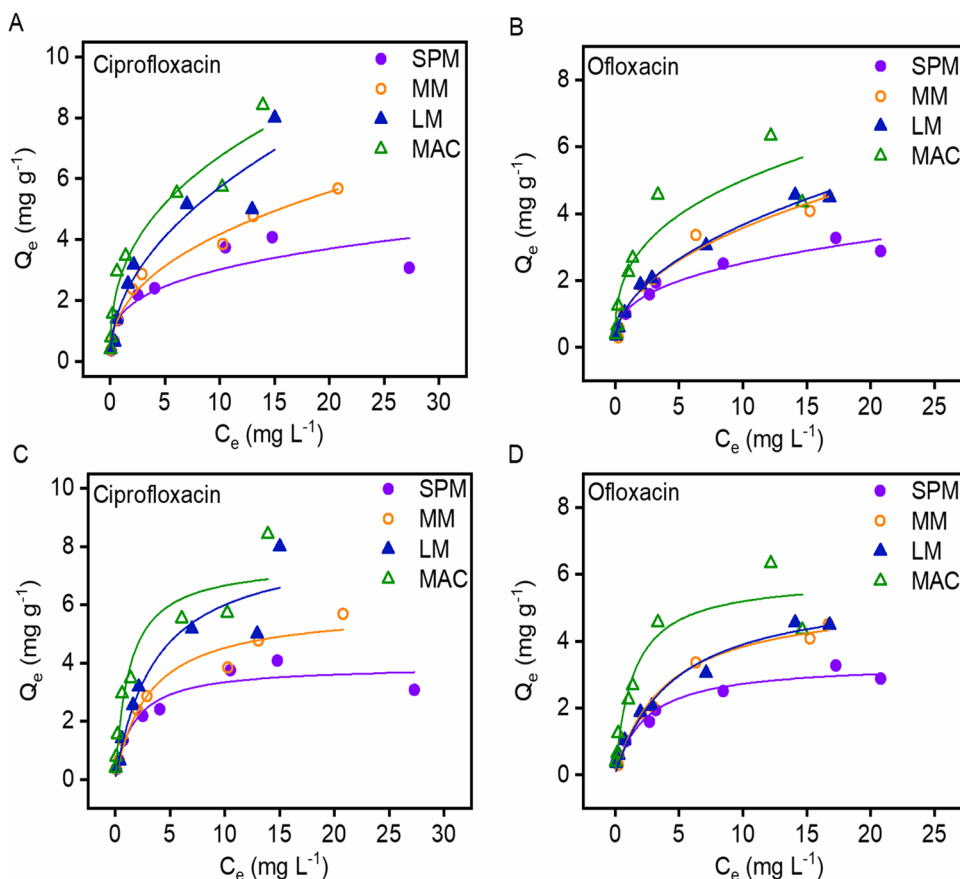
Effect of temperature and adsorption thermodynamics

The effects of temperature on the adsorption of CPX and OFL on different sediment aggregation fractions are shown in Fig. S1-S2, and Fig. 4. The temperature significantly influenced the amount of CPX and OFL

adsorbed by sediment fractions, and the saturated adsorption capacities (Q_e), irrespective of sediment aggregation fraction size, were gradually increased with the increasing temperature from 288.15 to 308.15 K. This positive effect of temperature might be due to the increased number of adsorption sites on sediment fractions with increasing temperature (Peng et al. 2015). Another possible explanation for this phenomenon is that the increased temperature of aqueous solution may decrease the resistance of two antibiotics entering into sediment aggregations, which in turn enhanced the adsorption capacity of sediments (Carrales-Alvarado et al. 2014). The Freundlich model could better explain the adsorption characteristics of different sediment aggregation fractions to the two antibiotics at different temperatures (Table 2).

The thermodynamic parameters are shown in Table 3. The ΔG values were negative, indicating that the adsorption of CPX and OFL onto the four sediment aggregations was spontaneous under standard conditions. The ΔH values for the adsorption of CPX and OFL onto sediment aggregation were positive (Table 3). The magnitude of ΔH values can give an idea whether the adsorption belongs to physisorption or chemisorption (Anggraini et al. 2014). In particular, when ΔH range from 2.1 to 10 $\text{kJ}\cdot\text{mol}^{-1}$, the

Fig. 4 Freundlich model (A, B) and Langmuir model (C, D) fitting the isothermal (298.15 K) adsorption of ciprofloxacin and ofloxacin on four sediment aggregation fractions (SPM: small and primary microaggregation, MM: medium microaggregation, LM: large microaggregation, MAC)



adsorption mechanism is physisorption, and when ΔH is in the range from 80 to 200 $\text{kJ}\cdot\text{mol}^{-1}$, the adsorption belongs to chemisorption (Li et al. 2011; Angraini et al. 2014). The ΔH values for CPX (11.437–41.239 $\text{kJ}\cdot\text{mol}^{-1}$), CPX (12.663–27.240 $\text{kJ}\cdot\text{mol}^{-1}$) indicate that the adsorption of CPX and OFL on four sediment aggregations could be attributed to the combination of physisorption and chemisorption rather pure physical or chemical adsorption. The positive values of ΔS implied that the freedom degree of two antibiotics at the solid-liquid interface increases during the adsorption process.

Competitive adsorption of CPX and OFL on different sediment aggregation fractions

When two antibiotics were added, the adsorption results (Q) of CPX and OFL on the sediment aggregation fraction, irrespective of the fraction size, increased with the increasing antibiotic concentrations, and all sediment aggregation fraction have stronger adsorption capability to the former one (Fig. 5). Figure 5 also illustrates the CPX was more easily adsorption than OFL. There was no difference in the Q of CPX and OFL, when the added concentration of antibiotics was below $2\text{ mg}\cdot\text{L}^{-1}$.

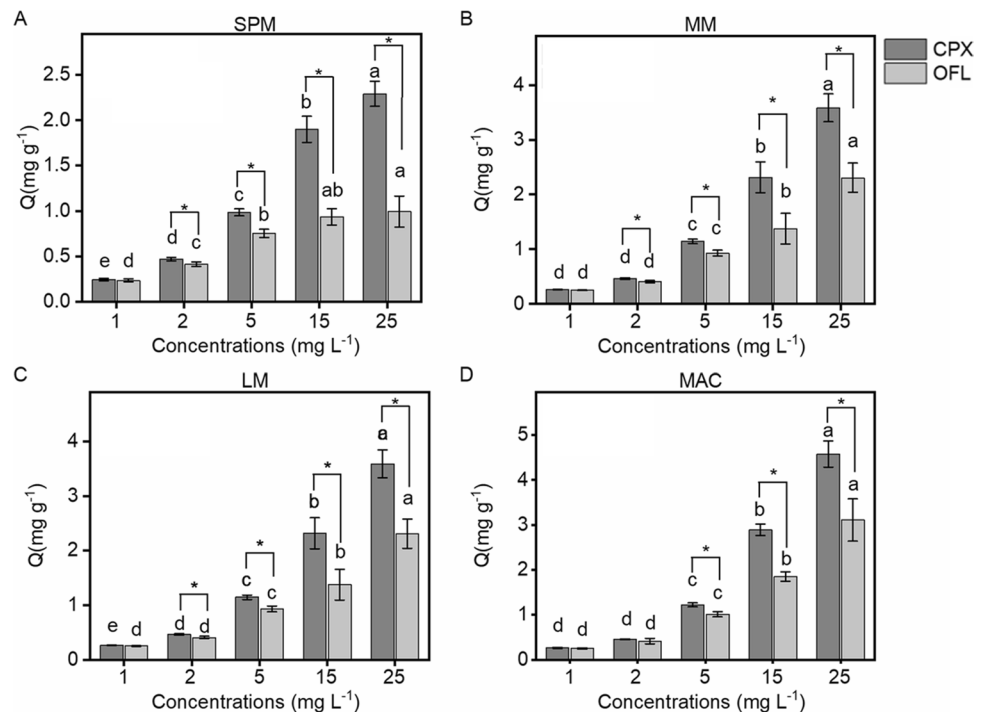
However, the Q became significant difference for two antibiotics, with the increasing added concentration. The Q of CPX for all sediment aggregation fractions were more than 10% higher than that of OFL (Fig. 5).

We compared the results of simple systems (existence of a single antibiotic) and binary systems (concurrent presence of two antibiotics) (Fig. S4). For CPX, in binary systems, all sediment aggregation fractions adsorption results (Q) were lower more than 23.4%, while Q was lower greater than 27.4% for OFL. We hypothesize that the CPX and OFL competed for adsorption sites on the aggregation surface and the CPX has a stronger affinity with sediment aggregation fraction, additionally, CPX and OFL have their unique adsorption sites. The decline in adsorption was more pronounced for OFL compared to CPX, demonstrating that the main competitive effect is associated with the affinity with the adsorbent for individual compounds (Mansouri et al. 2015). Conkle et al. (2010) also indicated that CPX is more advantageous when competing with OFL for the same adsorption site. Moreover, the physicochemical properties of the sediment aggregation fraction have a better affinity for CPX, which can also confirm that the sediment aggregation fractions adsorb most of CPX during competitive adsorption.

Table 3 Thermodynamic parameters for the adsorption of CPX and OFL

Antibiotic	Sediment fraction	T (K)	ΔG (kJ·mol ⁻¹)	ΔH (kJ·mol ⁻¹)	ΔS (kJ·mol ⁻¹ ·K ⁻¹)
Ciprofloxacin (CPX)	SPM (< 20 μm)	288.15	-0.445	41.239	0.144
		298.15	-1.061		
		308.15	-3.357		
	MM (20–63 μm)	288.15	-0.891	22.739	0.081
		298.15	-1.171		
		308.15	-2.545		
	LM (63–200 μm)	288.15	-0.206	11.437	0.045
		298.15	-0.531		
		308.15	-2.123		
	MAC (> 200 μm)	288.15	-1.415	12.234	0.049
		298.15	-2.064		
		308.15	-2.388		
Ofloxacin (OFL)	SPM (< 20 μm)	288.15	-0.712	27.240	0.096
		298.15	-0.344		
		308.15	-2.681		
	MM (20–63 μm)	288.15	-0.040	25.869	0.089
		298.15	-0.551		
		308.15	-1.848		
	LM (63–200 μm)	288.15	-1.777	27.191	0.094
		298.15	-1.579		
		308.15	-2.710		
	MAC (> 200 μm)	288.15	-1.943	12.663	0.049
		298.15	-2.582		
		308.15	-2.923		

Fig. 5 The adsorption content of were absorbed onto sediment aggregation 663 fractions (bars with different letters are significant differences among the antibiotic concentrations at $p < 0.05$ according to one-way ANOVA; * indicates significant difference between ciprofloxacin and ofloxacin at $p < 0.05$ according to Student's *t*-test; SPM: small and primary microaggregation, MM: medium microaggregation, LM: large microaggregation, MAC: microaggregation)



Analysis of EPS adsorption CPX and OFL

The growth of biofilms on the surface of sediment increases affects the distribution of hydrophobic organic pollutants on sediment (Wicke et al. 2008). EPS, as the main component of biofilms, was considered to play a positive role in adsorption organic pollutants. Studies have shown that EPS has a strong adsorption capacity for antibiotics like sulfadiazine and ofloxacin in water environments (Zhang et al. 2018; Wang et al. 2019). Nowadays, fluorescence quenching method has been successfully applied to characterize the physical or chemical processes between EPS and organic pollutants (Dong et al. 2017; Guo et al. 2020). However, the EPS composition is complex, and the spectra of different fluorophores tend to overlap, and EEM-PACAFAC can efficiently analyze the relationship between independent fluorescent components and organic pollutants (Xu et al. 2013).

EEM-PARAFAC analysis showed that three specific components (C1, C2, and C3) were identified in all original EPS extracted from four sediment aggregation fractions (Fig. 6A–C). The three fluorescent components were determined based on the similarity > 95% using the OpenFluor database (Murphy et al. 2014). C1 (Ex/Em = 270/375), C2 (Ex/Em = 270/300(355)) and C3 were classified as tryptophan protein-like component (Williams et al. 2010), tyrosine protein-like component (Li

et al. 2021c), and humic-like substances (Yamashita et al. 2011), respectively. The basis of the F_{\max} values indicates that protein-like substance is the major component of EPS in the sediment aggregation fraction (Table S4).

After adsorption of antibiotics by EPS in the sediment aggregation fractions adsorption antibiotics, C1-C3 of the initial EPS were not identified, only two new specific components (C4 and C5) were identified (Fig. 6D-E), the C4 and C5 can be associated with CPX (Fig. S5a) and OFL (Fig. S5b). It can be concluded that the three substances were occurred in fluorescence quenching after EPS adsorption two antibiotics. For C1 and C2, which belong to protein-like substances, one possible reason of quenching phenomenon was that the chemical structure of proteins in EPS would be damaged when exposure to high concentration of toxic substances (Miao et al. 2017). Another reason was that the amino and aromatic groups in the protein could be complexed with antibiotic (Fu et al. 2016). For C3, the reason for fluorescence quenching could also be the complexes formed by C3 and two antibiotics. Li et al. (2018a) reported that the aliphatic and aromatic series of humic-like substances could complex with sulfamethoxazole through various mechanisms, such as hydrogen and π - π bonding. Overall, EPS on the surface of different sediment aggregation fractions was capable of complexing reactions with two antibiotics.

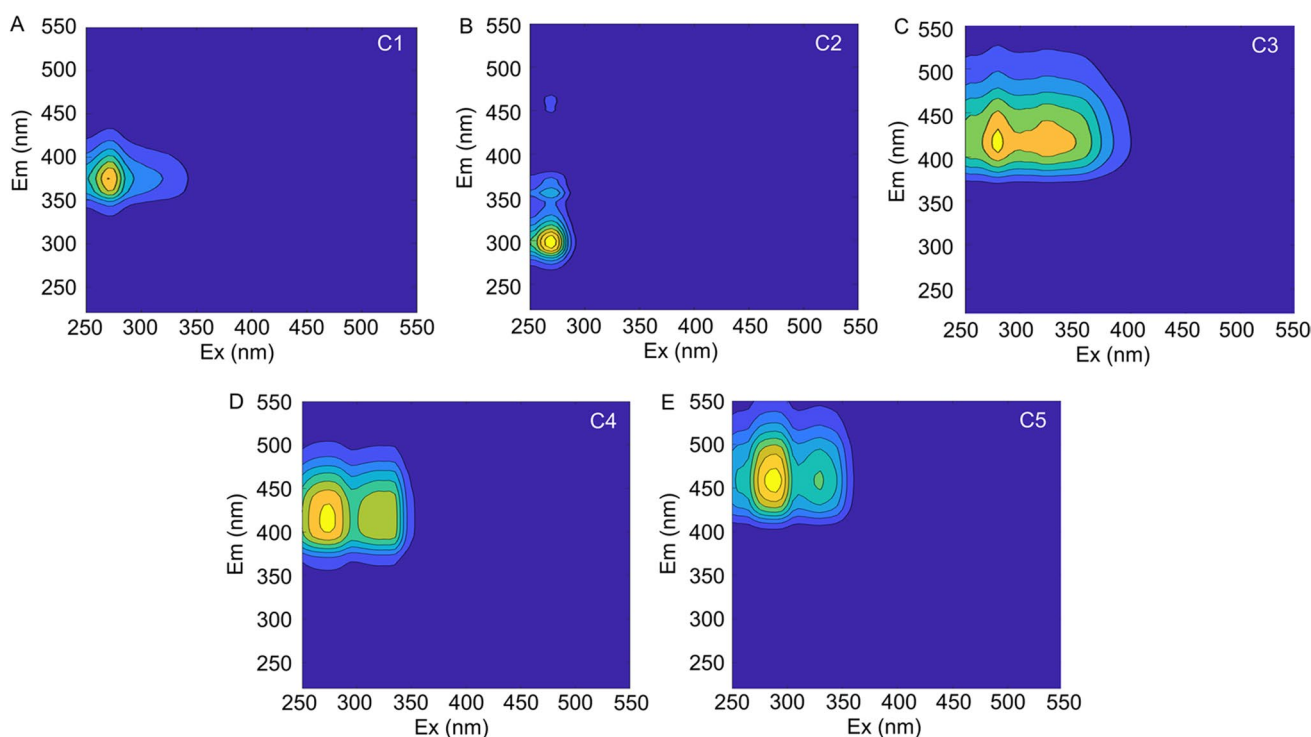
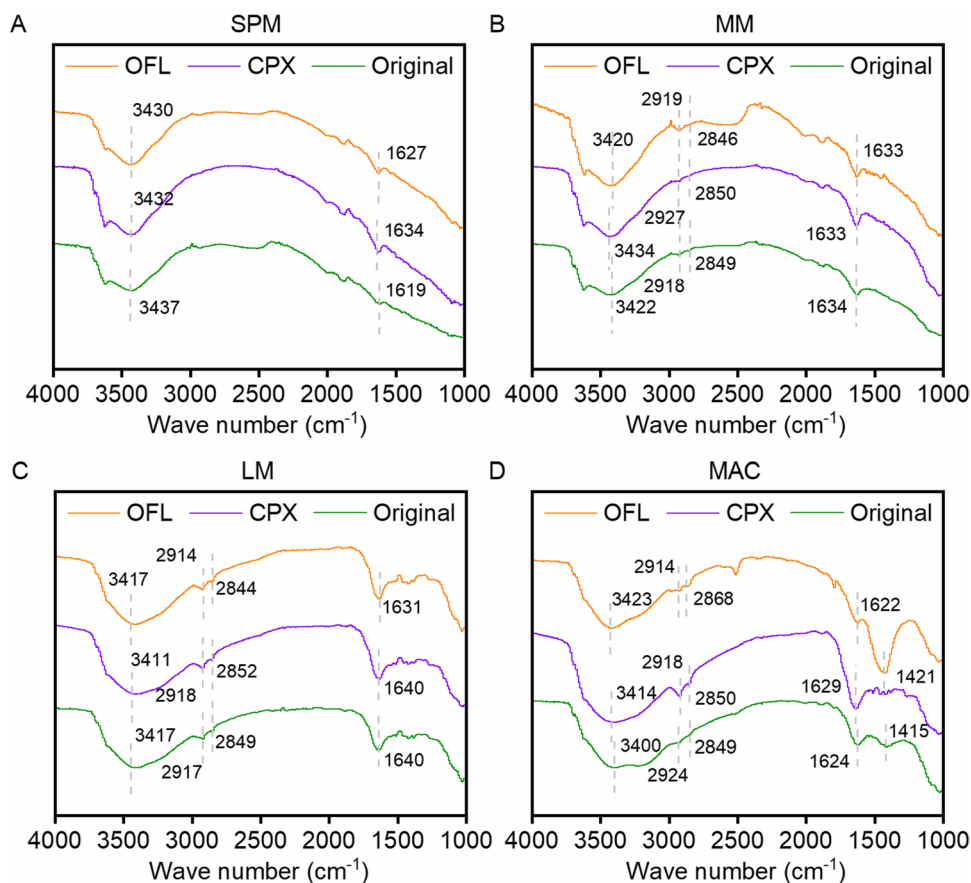


Fig. 6 Three-component fingerprints from the EEM-PARAFAC of original EPS (A, B, C) and after adsorption 668 CPX and OFL (D, E)

Fig. 7 Fourier transform infrared spectra of four sediment aggregate 669 fractions before antibiotic adsorption (original) and after ciprofloxacin (CPX) and ofloxacin (OFL) adsorption (SPM: small and primary microaggregation, MM: medium microaggregation, LM: large microaggregation, MAC: microaggregation)



Fourier-transform infrared analysis

To investigate the functional groups involved in the adsorption, the FTIR of two antibiotics (Fig. S6) and four sediment aggregation fractions before and after adsorption pollutants were measured (Fig. 7). The bands in FTIR spectra ranging from 3402 to 3436 cm^{-1} , from 2800 to 3000 cm^{-1} , from 1610 to 1640 cm^{-1} , and near 1420 cm^{-1} correspond to the stretching of the N–H bond of amino groups and the O–H bond of phenolic groups (Fu et al. 2016), C–H vibrations in aromatics (Singh and Srivastava 2020), C=O in the amide I band and C=C in aromatic rings (Chen et al. 2018), C–O asymmetric stretching carboxylic moieties (Bai et al. 2017). Before antibiotic adsorption, MAC mainly contained hydroxyl, carboxyl, amine and aliphatic CH, MM and LM mainly contained amine, carboxyl, and aliphatic CH, and SPM only contained hydroxyl, amine. This indicated that the functional group types on sediment aggregation fraction surface were fraction size-dependent.

Some bands in the FTIR spectra of all sediment aggregation fractions changed after adsorption CPX and OFL. With regard to all sediment aggregation fractions, the intensities of the bands at 3402 to 3436 cm^{-1} and 1610 to 1640 cm^{-1} all increased. These results indicated that the bands of O–H, N–H, C=O and C=C in four sediment

aggregation fractions were involved in the binding of CPX and OFL. The N–H and O–H on the surface of sediment aggregation fractions were π -electron-donor groups, and C=C was π -electron-acceptor group. Similarly, the molecular of two antibiotics has benzene ring and C=C with π -electron-acceptor groups, N–H with π -electron-donor group. Therefore, the sorption of two antibiotics by all fractions of sediment might be through π - π electron-donor–acceptor interactions. Duan et al. (2019) had reported that the O–H and N–H on the surface of sediment could provide a binding site for fluoroquinolones adsorption via π - π interaction. There are two C=O bands in the structure of two antibiotics, which are easily from hydrogen bonds with -COOH and O–H and N–H of sediment aggregation fractions. Thus, all sediment aggregation fractions adsorption might also adsorb CPX and OFL through forming hydrogen bonding. In previous study, hydrogen bonds were reported to readily form in the hydroxyl groups on the adsorbent surface (Jing et al. 2014). The characteristic band intensity of the MAC located at 1420 becomes stronger after adsorption of OFL, but disappeared after CPX adsorption (Zhao et al. 2019). This indicated that functional groups in the MAC were more likely to be complexed with carboxyl groups in CPX, and carboxyl groups in MAC were able to complex with amine groups in CPX.

Conclusion

This study showed that the adsorption behaviors of sediments to fluoroquinolones antibiotics were depended on sediment aggregation fraction and antibiotic type. Compared with the small sediment aggregation fraction, MAC had the stronger adsorption capacity to two fluoroquinolone antibiotics. While the adsorption of four sediment aggregation fractions to CPX and OFL, irrespective their fraction sizes, fitted the Freundlich model. The adsorption processes of sediment aggregation fractions to both CPX and OFL were dominated by chemical processes. Physicochemical properties of sediment aggregation (such as TOC, BET and CEC) contributed to the adsorption of CPX and OFL. EEM-PARAFAC and FTIR analysis shows that the organic matter on the surface of sediment could complexed with two antibiotics by π - π electron-donor-acceptor interactions and forming hydrogen bonding. Moreover, four sediment aggregation fractions were better affinity for CPX than OFL, and the functional groups in MAC were more likely to be complexed with carboxyl groups in CPX. This finding enhanced our understanding of migration and transport processes of antibiotics in aquatic sediment. More studies are needed to focus on predicting antibiotic migration in aquatic sediment.

Supplementary Information The online version contains supplementary material available at <https://doi.org/10.1007/s11356-022-23947-0>.

Author contribution Conceptualization: Bo Zhang; Writing – original draft preparation: Bo Zhang; Formal analysis and investigation: Bo Zhang, Juan Chen; Writing—review and editing: Juan Chen; Funding acquisition: Juan Chen, Peifang Wang; Project administration: Juan Chen, Peifang Wang; Methodology: Chao Wang, Ge Cui; Software: Juan Chen, Jingjing Zhang; Supervision: Chao Wang; Data curation: Ge Cui; Validation: Yu Hu; Visualization: Han Gao.

Funding This work was supported by the National Natural Science Foundation of China (No. 52022028, No. 52279061) and the Key Program of National Natural Science Foundation of China (No. 92047201, No. 92047303).

Data availability Not applicable.

Declarations

Ethical approval Not applicable.

Consent to participate Not applicable.

Consent for publication Not applicable.

Competing interests The authors declare no competing interests.

References

Aga DS, Lenczewski M, Snow D, Muurinen J, Sallach JB, Wallace JS (2016) Challenges in the measurement of antibiotics and in

- evaluating their impacts in agroecosystems: a critical review. *J Environ Qual* 45(2):407–419
- Aljeboree AM, Alshirifi AN, Alkaim AF (2017) Kinetics and equilibrium study for the adsorption of textile dyes on coconut shell activated carbon. *Arab J Chem* 10:S3381–S3393
- Almeida A, Duarte S, Nunes R, Rocha H, Pena A, Meisel L (2014) Human and veterinary antibiotics used in Portugal—a ranking for ecosurveillance. *Toxics* 2(2):188–225
- Anggraini M, Kurniawan A, Ong LK, Martin MA, Liu JC, Soetaredjo FE, ... Ismadji S (2014) Antibiotic detoxification from synthetic and real effluents using a novel MTAB surfactant-montmorillonite (organoclay) sorbent. *RSC Adv* 4(31), 16298–16311
- Arshadi M, Eskandarloo H, KarimiAbdolmaleki M, Abbaspourrad A (2018) A biocompatible nanodendrimer for efficient adsorption and reduction of Hg(II). *ACS Sustain Chem Eng* 6(10):13332–13348
- Bai L, Zhao Z, Wang C, Wang C, Liu X, Jiang H (2017) Multi-spectroscopic investigation on the complexation of tetracycline with dissolved organic matter derived from algae and macrophyte. *Chemosphere* 187:421–429
- Binh VN, Dang N, Anh NTK, Le XK, Thai PK (2018) Antibiotics in the aquatic environment of vietnam: sources, concentrations, risk and control strategy. *Chemosphere* 197:438–450
- Carrales-Alvarado DH, Ocampo-Pérez R, Leyva-Ramos R, Rivera-Utrilla J (2014) Removal of the antibiotic metronidazole by adsorption on various carbon materials from aqueous phase. *J Colloid Interf Sci* 436:276–285
- Cao E, Duan W, Wang A, Zheng Y (2017) Oriented growth of poly(m-phenylenediamine) on *Calotropis gigantea* fiber for rapid adsorption of ciprofloxacin. *Chemosphere* 171:223–230
- Chen J, Wang P, Wang C, Wang X, Miao L, Liu S, Yuan Q, Sun S (2020) Fungal community demonstrates stronger dispersal limitation and less network connectivity than bacterial community in sediments along a large river. *Environ Microbiol* 22(3):832–849
- Chen Y, Lin Y, Ho S, Zhou Y, Ren N (2018) Highly efficient adsorption of dyes by biochar derived from pigments-extracted macroalgae pyrolyzed at different temperature. *Bioresour Technol* 259:104–110
- Conde-Cid M, Ferreira-Coelho G, Núez-Delgado A, Fernández-Calvino D, Arias-Estévez M, Álvarez-Rodríguez E, Fernández-Sanjurjo MJ (2019) Competitive adsorption of tetracycline, oxytetracycline and chlortetracycline on soils with different pH value and organic matter content. *Environ Res* 178, 108669
- Conkle JL, Latta C, White JR, Cook RL (2010) Competitive sorption and desorption behavior for three fluoroquinolone antibiotics in a wastewater treatment wetland soil. *Chemosphere* 80(11):1353–1359
- Dinh QT, Moreau-Guigon E, Pierre L, Fabrice A, Marie-Jeanne T, Martine B, Joelle E, Marc C (2017) Fate of antibiotics from hospital and domestic sources in a sewage network. *Sci Total Environ* 575:758–766
- Dong D, Zhang L, Guo Z, Hua X (2017) The role of extracellular polymeric substances on the sorption of pentachlorophenol onto natural biofilms in different incubation times: a fluorescence study. *Chem Ecol* 33(2):131–142
- Duan W, Li M, Xiao W, Wang N, Niu B, Zhou L, Zheng Y (2019) Enhanced adsorption of three fluoroquinolone antibiotics using polypyrrole functionalized *Calotropis gigantea* fiber. *Colloid Surface a* 574:178–187
- Fadário VMF, Dias M, Teixeira ACSC, Alves Palma MSA (2014) Environmental contamination by fluoroquinolones. *Braz J Pharm Sci* 50:41–54
- Fan C, Zhang L, Qin B, Wang S, Hu W, Zhang C (2004) Estimation on dynamic release of phosphorus from wind-induced suspended particulate matter in Lake Taihu. *Sci China Ser D* 478:710–719

- Fu Q, He J, Blaney L, Zhou D (2016) Roxarsone binding to soil-derived dissolved organic matter, insights from multi-spectroscopic techniques. *Chemosphere* 155:225–233
- Gu C, Gao P, Yang F, An D, Munir M, Jia H, Xue G, Ma C (2017) Characterization of extracellular polymeric substances in biofilms under long-term exposure to ciprofloxacin antibiotic using fluorescence excitation-emission matrix and parallel factor analysis. *Environ Sci Pollut Res* 24(15):13536–13545
- Guo Y, Qin P, Wang C, Pan X, Dong X, Zong W (2020) Characterization on the toxic mechanism of two fluoroquinolones to trypsin by spectroscopic and computational methods. *J Environ Sci Heal B* 55(3):230–238
- Han S, Delgado-Baquerizo M, Luo X, Liu Y, Van Nostrand JD, Chen W, Zhou J, Huang Q (2021) Soil aggregate size-dependent relationships between microbial functional diversity and multifunctionality. *Soil Biol Biochem* 154:108143
- Hanamoto S, Nakada N, Jürgens MD, Johnson AC, Yamashita N, Tanaka H (2018) The different fate of antibiotics in the Thames River, UK, and the Katsura River. *Japan Environ Sci Pollut Res* 25(2):1903–1913
- Hu Y, Pan C, Zheng X, Liu S, Hu F, Xu L ... Peng X (2020) Removal of ciprofloxacin with aluminum-pillared kaolin sodium alginate beads (CA-Al-KABs): Kinetics, isotherms, and BBD model. *Water* 12(3), 905
- Huang M, Li Z, Huang B, Luo N, Zhang Q, Zhai X, Zeng G (2018) Investigating binding characteristics of cadmium and copper to DOM derived from compost and rice straw using EEM-PARAFAC combined with two-dimensional FTIR correlation analyses. *J Hazard Mater* 344:539–548
- Huang Y, Wang Y, Huang Y, Zhang L, Ye F, Wang J, Shang J, Liao Q (2020) Impact of sediment characteristics on adsorption behavior of typical antibiotics in Lake Taihu. *China Sci Total Environ* 718:137329
- Jing XR, Wang YY, Liu WJ, Wang YK, Jiang H (2014) Enhanced adsorption performance of tetracycline in aqueous solutions by methanol-modified biochar. *Chem Eng J* 248:168–174
- Klein EY, Van Boeckel TP, Martinez EM, Pant S, Gandra S, Levin SA, Goossens H, Laxminarayan R (2018) Global increase and geographic convergence in antibiotic consumption between 2000 and 2015. *Proc Natl Acad Sci USA* 115(15):E3463–E3470
- Kovalakova P, Cizmas L, McDonald TJ, Marsalek B, Feng M, Sharma VK (2020) Occurrence and toxicity of antibiotics in the aquatic environment: a review. *Chemosphere* 251:126351
- Li J, Sabourin L, Renaud J, Halloran S, Singh A, Sumarah M, Dagnew M, Ray MB (2021a) Simultaneous quantification of five pharmaceuticals and personal care products in biosolids and their fate in thermo-alkaline treatment. *J Environ Manage* 278:111404
- Li L, Zhao X, Liu D, Song K, Liu Q, He Y (2021b) Occurrence and ecological risk assessment of PPCPs in typical inflow rivers of Taihu lake. *China J Environ Manage* 285:112176
- Li J, Liao L, Jia Y, Tian T, Gao S, Zhang C, ... Wang Z (2022) Magnetic Fe₃O₄/ZIF-8 optimization by Box-Behnken design and its Cd (II)-adsorption properties and mechanism. *Arab. J. Chem.* 15(10), 104119
- Li S, Ju H, Ji M, Zhang J, Song K, Chen P, Mu G (2018a) Terrestrial humic-like fluorescence peak of chromophoric dissolved organic matter as a new potential indicator tracing the antibiotics in typical polluted watershed. *J Environ Manage* 228:65–76
- Li S, Shi W, Liu W, Li H, Zhang W, Hu J, Ke Y, Sun W, Ni J (2018b) A duodecennial national synthesis of antibiotics in China's major rivers and seas (2005–2016). *Sci Total Environ* 615:906–917
- Li X, Zhou X, Mu J, Lu L, Han D, Lu C, Wang M (2011) Thermodynamics and kinetics of p-aminophenol adsorption on poly (aryl ether ketone) containing pendant carboxyl groups. *J Chem Eng Data* 56(11):4274–4277
- Li Y, Zhang Y, Li Z, Wan J, Dang C, Fu J (2021c) Characterization of colored dissolved organic matter in the northeastern South China Sea using EEMs-PARAFAC and absorption spectroscopy. *J Sea Res* 180:102159
- Li Z, Li M, Zhang Z, Li P, Zang Y, Liu X (2020) Antibiotics in aquatic environments of China: a review and meta-analysis. *Ecotox Environ Safe* 199(11):110668
- Luo Y, Chen J, Wu C, Zhang J, Tang J, Shang J, Liao Q (2019) Effect of particle size on adsorption of norfloxacin and tetracycline onto suspended particulate matter in lake. *Environ Pollut* 244:549–559
- Maged A, Kharbush S, Ismael IS, Bhatnagar A (2020) Characterization of activated bentonite clay mineral and the mechanisms underlying its sorption for ciprofloxacin from aqueous solution. *Environ Sci Pollut Res* 27(26):32980–32997
- Mansouri H, Carmona RJ, Gomis-Berenguer A, Souissi-Najar S, Ouederni A, Ania CO (2015) Competitive adsorption of ibuprofen and amoxicillin mixtures from aqueous solution on activated carbons. *J Colloid Interf Sci* 449:252–260
- Marttila H, Kløve B (2015) Spatial and temporal variation in particle size and particulate organic matter content in suspended particulate matter from peatland-dominated catchments in Finland. *Hydrol Process* 29(6):1069–1079
- Miao L, Wang C, Hou J, Wang P, Ao Y, Li Y, Yao Y, Lv B, Yang Y, You G, Xu Y, Gu Q (2017) Response of wastewater biofilm to CuO nanoparticle exposure in terms of extracellular polymeric substances and microbial community structure. *Sci Total Environ* 579:588–597
- Murphy KR, Stedmon CA, Wenig P, Bro R (2014) OpenFluor—an online spectral library of auto-fluorescence by organic compounds in the environment. *Anal Methods-UK* 6(3):658–661
- Parente CET, Brito EMS, Azeredo A, Meire RO, Malm O (2019) Fluoroquinolone antibiotics and their interactions in agricultural soils—a review. *Orbital* 11(1):42–52
- Pezoti Jr O, Cazetta AL, Souza IP, Bedin KC, Martins AC, Silva TL, Almeida VC (2014) Adsorption studies of methylene blue onto ZnCl₂-activated carbon produced from buriti shells (*Mauritia flexuosa* L.). *J Ind Eng Chem* 20(6), 4401–4407
- Peng X, Hu F, Lam FL, Wang Y, Liu Z, Dai H (2015) Adsorption behavior and mechanisms of ciprofloxacin from aqueous solution by ordered mesoporous carbon and bamboo-based carbon. *J Colloid Interf Sci* 460:349–360
- Philip JM, Aravind UK, Aravindakumar CT (2018) Emerging contaminants in Indian environmental matrices—a review. *Chemosphere* 190:307–326
- Qi Y, Zhang TC, Ren Y (2014) Testosterone sorption and desorption: effects of soil particle size. *J Hazard Mater* 279, 493–501
- Rath S, Fostier AH, Pereira LA, Dioniso AC, Ferreira FD, Doretto KM, Peruchi LM, Viera A, Neto OFD, Dal Bosco SM, Martínez-Mejía MJ (2019) Sorption behaviors of antimicrobial and antiparasitic veterinary drugs on subtropical soils. *Chemosphere* 214:111–122
- Sangster JL, Oke H, Zhang Y, Bartelt-Hunt SL (2015) The effect of particle size on sorption of estrogens, androgens and progestagens in aquatic sediment. *J Hazard Mater* 299:112–121
- Scherr FF, Sarmah AK, Di HJ, Cameron KC (2009) Sorption of estrone and estrone-3-sulfate from CaCl₂ solution and artificial urine in pastoral soils of New Zealand. *Environ Toxicol Chem* 28(12):2564–2571
- Shen S, Yang S, Jiang Q, Luo M, Li Y, Yang C, Zhang D (2020) Effect of dissolved organic matter on adsorption of sediments to Oxytetracycline: an insight from zeta potential and DLVO theory. *Environ Sci Pollut Res* 27(2):1697–1709
- Siebers N, Abdelrahman H, Krause L, Amelung W (2018) Bias in aggregate geometry and properties after disintegration and drying procedures. *Geoderma* 313:163–171

- Siedlewicz G, Bialk-Bielinska A, Borecka M, Winogradow A, Stepnowski P, Pazdro K (2018) Presence, concentrations and risk assessment of selected antibiotic residues in sediments and near-bottom waters collected from the Polish coastal zone in the southern Baltic Sea - Summary of 3 years of studies. *Mar Pollut Bull* 129(2):787–801
- Singh V, Srivastava VC (2020) Self-engineered iron oxide nanoparticle incorporated on mesoporous biochar derived from textile mill sludge for the removal of an emerging pharmaceutical pollutant. *Environ Pollut* 259:113822
- Six J, Elliott ET, Paustian K, Doran JW (1998) Aggregation and soil organic matter accumulation in cultivated and native grassland soils. *Soil Sci Soc Am J* 62(5):1367–1377
- Soltani R, Dinari M, Mohammadnezhad G (2018) Ultrasonic-assisted synthesis of novel nanocomposite of poly(vinyl alcohol) and amino-modified MCM-41: a green adsorbent for Cd(II) removal. *Ultrason Sonochem* 40:533–542
- Stedmon CA, Bro R (2008) Characterizing dissolved organic matter fluorescence with parallel factor analysis: a tutorial. *Limnol Oceanogr Meth* 6(11):572–579
- Tang J, Wang S, Fan J, Long S, Wang L, Tang C, Tam NF, Yang Y (2019) Predicting distribution coefficients for antibiotics in a river water-sediment using quantitative models based on their spatiotemporal variations. *Sci Total Environ* 655:1301–1310
- Tan F, Sun D, Gao J, Zhao Q, Wang X, Teng F ... Chen J (2013) Preparation of molecularly imprinted polymer nanoparticles for selective removal of fluoroquinolone antibiotics in aqueous solution. *J Hazard Mater* 244, 750-757
- Wang H, Hu C, Shen Y, Shi B, Zhao D, Xing X (2019) Response of microorganisms in biofilm to sulfadiazine and ciprofloxacin in drinking water distribution systems. *Chemosphere* 218:197–204
- Wicke D, Böckelmann U, Reemtsma T (2008) Environmental influences on the partitioning and diffusion of hydrophobic organic contaminants in microbial biofilms. *Environ Sci Technol* 42(6):1990–1996
- Williams CJ, Yamashita Y, Wilson HF, Jaffé R, Xenopoulos MA (2010) Unraveling the role of land use and microbial activity in shaping dissolved organic matter characteristics in stream ecosystems. *Limnol Oceanogr* 55(3):1159–1171
- Wu W, Zhou D (2019) Influence of biochar aging on its physicochemical properties and adsorption of heavy metals. *J Agro-Environ Sci* 38(1):7–13
- Xiong C, Xue C, Huang L, Hu P, Fan P, Wang S, Zhou X, Yang Z, Wang Y, Ji H (2021) Enhanced selective removal of Pb(II) by modification low-cost bio-sorbent: experiment and theoretical calculations. *J Clean Prod* 316:128372
- Xu J, Sheng G, Ma Y, Wang L, Yu H (2013) Roles of extracellular polymeric substances (EPS) in the migration and removal of sulfamethazine in activated sludge system. *Water Res* 47(14):5298–5306
- Xu J, Zhang Y, Zhou C, Guo C, Wang D, Du P, Luo Y, Wan J, Meng W (2014) Distribution, sources and composition of antibiotics in sediment, overlying water and pore water from Taihu Lake, China. *Sci Total Environ* 497:267–273
- Yamashita Y, Kloppel BD, Knoepp J, Zausen GL, Jaffé R (2011) Effects of watershed history on dissolved organic matter characteristics in headwater streams. *Ecosystems* 14(7):1110–1122
- Yang J, Huang Y, Chen Y, Hassan M, Zhang X, Zhang B, Gin KYH, He Y (2020) Multi-phase distribution, spatiotemporal variation and risk assessment of antibiotics in a typical urban-rural watershed. *Ecotox Environ Safe* 206:111156
- Yang L, Xiao S, Luan T, Tam NF (2018) Overproduction of microbial extracellular polymeric substances in subtropical intertidal sediments in response to endocrine disrupting chemicals. *Sci Total Environ* 624:673–682
- Yu K, Sun C, Zhang B, Hassan M, He Y (2019) Size-dependent adsorption of antibiotics onto nanoparticles in a field-scale wastewater treatment plant. *Environ Pollut* 248:1079–1087
- Zhang L, Dong D, Hua X, Guo Z (2018) Inhibitory effects of extracellular polymeric substances on ofloxacin sorption by natural biofilms. *Sci Total Environ* 625:178–184
- Zhao J, Liang G, Zhang X, Cai X, Li R, Xie X, Wang Z (2019) Coating magnetic biochar with humic acid for high efficient removal of fluoroquinolone antibiotics in water. *Sci Total Environ* 688:1205–1215
- Zhao T, Li X, Ning Z, Zhao H, Zhang J, Zhao W (2018) Pore structure and adsorption behavior of shale gas reservoir with influence of maturity: a case study of Lower Silurian Longmaxi formation in China. *Arab J Geosci* 11(13):1–4
- Zhao Y, Tan Y, Guo Y, Gu X, Wang X, Zhang Y (2013) Interactions of tetracycline with Cd (II), Cu (II) and Pb (II) and their cosorption behavior in soils. *Environ Pollut* 180:206–213
- Zheng W, Zhao Z, Gong Q, Zhai B, Li Z (2018) Responses of fungal-bacterial community and network to organic inputs vary among different spatial habitats in soil. *Soil Biol Biochem* 125:54–63
- Zhu Y, Bai Z, Wang B, Zhai L, Luo W (2017) Microfluidic synthesis of renewable biosorbent with highly comprehensive adsorption performance for copper (II). *Front Chem Sci Eng* 11(2):238–251

Publisher's note Springer Nature remains neutral with regard to jurisdictional claims in published maps and institutional affiliations.

Springer Nature or its licensor (e.g. a society or other partner) holds exclusive rights to this article under a publishing agreement with the author(s) or other rightsholder(s); author self-archiving of the accepted manuscript version of this article is solely governed by the terms of such publishing agreement and applicable law.